

# UNIFIED MODEL OF RADIO AND X-RAY EMISSION OF NOVA CI CAM 1998

N. N. Chugai

*Institute of Astronomy, RAS, Pyatnitskaya 48, 109017 Moscow, Russia*

nchugai@inasan.ru

## ABSTRACT

A unified model is proposed for the radio and X-ray outburst of nova CI Cam 1998 which suggests the shock interaction of nova shell with the circumstellar gas. The spherical model is able to describe kinematics of the radio shell together with the evolution of the radio and X-ray fluxes. However, the X-ray spectrum in this model is harder than the observed one. Better agreement with observations demonstrates the model in which the spherical shell interacts with the nonspherical circumstellar medium. The latter is made up of the broad bipolar jets with the opening angle of  $120^\circ$  and the dense equatorial wind. In the optimal model the kinetic energy of the nova shell is  $\sim 8 \times 10^{43}$  erg, while the shell mass lies in the range of  $(1 - 5) \times 10^{-7} M_\odot$ .

## 1. Introduction

Nova CI Cam was discovered 1998 March 31.64 by the ASM detector of *RXTE* as an X-ray outburst with the flux of 139 mCrab in the range 2-12 keV (Smith et al. 1998; Revnivtsev et al. 1999). At the earlier epoch March 31.36 this source was absent with the upper limit of 40 mCrab. The extrapolation of the flux evolution backwards results in the outburst moment March 31.5, i.e., 50903.5 MJD; this is considered below as zero point of the nova shell expansion. The X-ray source was identified with the binary of symbiotic type CI Cam (Wegner & Starrfield 1998), in which the luminosity is dominated by B-giant classified as B4 III-V[e] (Barsukova et al. 2006). The binary has the orbital period of 19.4 d, eccentricity  $e = 0.62$  and major semiaxis  $a = 4.8 \times 10^{12} / \sin i$  cm, where  $i$  is the inclination angle (Barsukova et al. 2006). The optical outburst was observed starting from April 3 at the decline stage with the exponential time of 3.4 d (Garcia et al. 1998; Clark et al. 2000).

Nova CI Cam 1998 turned out to be a bright source of the radio emission that was observed on several frequencies starting from April 1.9 (Hjelming 1998; Mioduszewski & Rupen

2004). The source mapping in radio band during several consecutive epochs starting from the beginning shows the source expansion with the velocity of  $\sim 12000 \text{ km s}^{-1}$  assuming the distance of 5 kpc (Mioduszewski & Rupen 2004). The radio emission is interpreted as a synchrotron emission of the shock wave propagating in the circumstellar medium (CSM). The radio evolution shows the strong early absorption at 2 GHz which can be caused by the synchrotron self-absorption (SSA) or/and  $ff$ -absorption in the CS gas (Mioduszewski & Rupen 2004). At the late stage  $t \sim 80 \text{ d}$  the radio shell shows an oval shape which is interpreted as a bipolar structure which can be interpreted as a prolate spheroid, bipolar jets, or bipolar spherical clouds (Mioduszewski & Rupen 2004). Interestingly, in this regard, (Filippova et al. 2008) note that the spherical shock wave in the wind predicts significantly slower decay of the the X-ray emission compared with observations and that the better agreement shows the model of the shock wave in the equatorial disk.

The nature of the unseen stellar component of CI Cam and the origin of the outburst are unclear. There is a conjecture that nova CI Cam is the result of the outburst in the binary containing black hole or neutron star (Frontera et al. 1998; Belloni et al. 1999). On the other hand there are serious arguments that unseen component is the white dwarf (WD) and that the nova CI Cam 1998 is the result of the thermonuclear explosion on the surface of the white dwarf as in classical novae (Ishida et al. 2004; Barsukova et al. 2006; Filippova et al. 2008).

Keeping in mind unusual nature of nova CI Cam it is desirable to advance in the interpretation of data on the radio and X-ray outbursts. Particularly it would be of interest to construct a model of the interaction of the nova shell with the CS gas that might account for the radio and X-ray data simultaneously. Such unified model possibly might provide us with interesting estimates of the crucial parameters, e.g., energy and mass of the nova shell. The radio and X-ray data indicate the possibility of the nonspherical distribution of the CSM. It would be sensible, therefore, to explore both spherical and nonspherical version of the model. This paper presents an attempt of the construction of the unified model in the framework of spherical and nonspherical approaches.

Model parameters essentially depend on the adopted distance ( $d$ ) which is poorly known. Most popular are two options:  $d = 2 \text{ kpc}$  (Clark et al. 2000; Filippova et al. 2008) and  $d = 5 \text{ kpc}$  (Mioduszewski & Rupen 2004; Ishida et al. 2004). I will present results for both distance choices.

## 2. Dynamical model

The basic model suggests the shock interaction of a spherical nova shell with a spherical CS medium. This model with some modification can be also used in the nonspherical case. Because the mechanism of the initial energy release is not completely clear, there is some uncertainty in the initial density and velocity distribution along the radius in the nova shell. Two mechanisms of the shell ejection are conceivable: an explosion which suggests the energy release on time scale less or comparable to hydrodynamic time scale and a relatively slow matter acceleration by the pressure gradient (optically thick wind). The latter is a major mechanism for the mass loss in classic novae (Prialnik 1986; Kato & Hachisu 1994). In case of CI Cam this mechanism however cannot explain the high expansion velocity of the radio source which exceeds  $5000 \text{ km s}^{-1}$  for the distance  $\geq 2 \text{ kpc}$  (Mioduszewski & Rupen 2004). I therefore assume that the nova shell was ejected explosively. In this case one expects that the shell expands homologously soon after the passage of the shock wave, i.e., in the time of  $\sim 10^2 \text{ s}$ . However, this does not specify the density distribution. Moreover, we do not know the matter distribution in the close vicinity of the white dwarf that could modify the initial density distribution of the nova shell.

Bearing in mind above uncertainties it is reasonable to use a most simple dynamic model in order to minimize the number of free parameters; the Sedov point explosion model is most appropriate. However one has to take into account also the initial deceleration phase. Indeed, even for the low mass ejecta  $\sim 3 \times 10^{-7} M_{\odot}$  expanding in the dense CSM  $n \sim 10^{10} \text{ cm}^{-3}$  the deceleration length scale is large  $R \sim 2 \times 10^{13} \text{ cm}$  with the corresponding time scale of  $\sim R/v \sim 1 \text{ d}$ . The deceleration phase is taken into account assuming the nova shell brakes as a whole with the energy conservation. Equations of the energy and mass conservation is solved by Runge-Kutta forth order method.

Note, the formulated deceleration problem for the shell of mass  $M_0$  and the energy  $E_0 = (1/2)M_0v_0^2$  expanding in the stationary wind with the density  $\rho = w/4\pi r^2$  can be solved analitically

$$r = r_s \left[ \left( \frac{t}{t_s} + 1 \right)^{2/3} - 1 \right], \quad (1)$$

where  $r_s = M_0/w$  is the radius at which the mass of the swept up shell becomes equal to the initial shell mass, and  $t_s = (2/3)r_s/v_0$ . At times  $t \gg t_s$  this solution approaches Sedov solution  $r \propto t^{2/3}$ . For  $M_0 = 3 \times 10^{-7} M_{\odot}$ , and wind density parameter  $w = 10^{13} \text{ g cm}^{-1}$  the characteristic radius is  $r_s = 6 \times 10^{13} \text{ cm}$ . For the initial velocity  $v_0 = 6000 \text{ km s}^{-1}$  the expansion enters the Sedov stage after about one day. The equation (1) is used to test numerical solution.

Following Filippova et al. (2008) I adopt the CSM distribution presented by a homogeneous core and an outer stationary wind. Specifically,  $\rho = \rho_0 = \text{const}$  in the inner zone  $r < r_0 = 2 \times 10^{13}$  cm and  $\rho = \rho_0(r/r_0)^{-2}$  for  $r > r_0$ . The homogeneous core approximately takes into account the orbital motion of the less massive component with the velocity of  $\approx 230$  km s $^{-1}$  which affects the slow wind flow with the velocity of  $u = 32$  km s $^{-1}$  (Robinson et al. 2002) in the orbital zone  $r \sim 10^{13}$  cm. In fact, computations show that the shell dynamics only weakly depends on the variations of the density distribution in the region  $r < r_0$ .

A large volume of the parameter space was explored; below only two versions of the spherically-symmetric model are presented. They correspond to the minimal energy for which we are able to describe the expansion kinematics of the radio shell and to reproduce maximal X-ray flux for the adopted distance. The shell mass is poorly constrained because the expansion dynamics and X-ray ray emission are sensitive primarily to the energy and the CS density, not to the shell mass. In the model A for  $d = 2$  kpc and the energy  $1.1 \times 10^{44}$  erg the shell mass lies in the range  $(1 - 5) \times 10^{-7} M_\odot$  with the accepted optimal value of  $2 \times 10^{-7} M_\odot$  defined by the radius of the radio source at the age  $t \sim 2$  d. In the model B for  $d = 5$  kpc with  $E = 1.6 \times 10^{45}$  erg I adopt the same mass  $2 \times 10^{-7} M_\odot$ . Models parameters are listed in Table 1 which, starting from the second column, shows the distance, shell mass and energy, CS density in the central zone,  $r < r_0$ , parameter of the density of the relativistic energy  $\epsilon_r$ , spectral index of the relativistic electrons, and the filling factor of the radio-emitting clouds. The sense of some parameters is described in the appropriate place below.

The evolution of the shock wave radius for the models A and B (Fig. 1 and Table 1) satisfactorily reproduces the observed expansion of the radio source at the time scale of  $\sim 10^2$  d. The initial velocity in the model A is 7400 km s $^{-1}$ , somewhat larger than maximal velocities of novae shells but still within escape velocities  $\approx 1.1 \times 10^4$  km s $^{-1}$  for white dwarfs with masses  $\sim 1.3 M_\odot$  (Althaus et al. 2005). In the model B with  $d = 5$  kpc the initial velocity  $2.8 \times 10^4$  km s $^{-1}$  is significantly larger than the velocity expected for any known type of cataclismic system with the white dwarf.

### 3. X-ray emission of the shock wave

In our model the reverse shock is absent. Fortunately, the role of the reverse shock in the X-ray emission is negligible: it is important only at the early deceleration stage  $t \sim 1$  d. Moreover even at this stage it contributes only in the soft band  $< 1$  keV (Filippova et al. 2009) because the speed of the reverse shock is relatively low. The X-ray emission of the forward shock is calculated assuming a homogeneous density of the shocked gas. The shock speed is assumed to be equal to the shell velocity found from the dynamics computation.

The post-shock density is determined assuming strong shock limit. The contribution of the relativistic pressure (relativistic particles plus magnetic field) with a fraction  $\eta$  of the total pressure is taken into account. The compression factor in this case is  $4 + 3\eta$  (Chevalier 1983). The inclusion of the relativistic pressure requires the iterative procedure: at the first step we compute dynamics and X-ray emission; afterwards we calculate radio emission which provides us with the estimate of  $\eta$  and then again recalculate X-ray emission. The electron temperatures is calculated from the equation of the heat exchange between ions and electrons  $dT_e/dt = T_i/t_{eq}$ , where  $t_{eq} = CT_e^{3/2}/n_i$  is equilibration time,  $n_i$  is the ion concentration,  $C$  is the factor specified in (Spitzer 1962). The initial temperatures in the shock  $T_e$  and  $T_i$  are taken according to Rankine-Hugoniot jump conditions while the age is adopted as an integration interval. The cooling function is taken according to Sutherland & Dopita (1993). The X-ray flux density is presented by the spectrum  $F(E) \propto E^{-0.5} \exp(-E/T)$  (where  $E$  and  $T$  are in keV). Calculations show that always  $T_e < T_i$ .

The model unabsorbed flux in the range of 3 – 20 keV is shown in Fig. 2 together with the unabsorbed flux derived from observations (Filippova et al. 2008). Insets show the evolution of the computed  $T_e$  compared to the electron temperature recovered from the observed spectrum (Filippova et al. 2008). The flux in the model A is consistent with observations only around maximum during the first day; afterwards the flux decays more slowly than the observed one. The similar behavior shows the model flux in the paper (Filippova et al. 2008). The temperature significantly exceeds the observed one (Fig. 2) which reflects higher shock speed than is needed to account for the X-ray spectrum of CI Cam 1998. In the model B we face the same problem of the slow flux evolution as in model A, while the temperature shows even larger deviation from the observed one compared to model A. This difference is related with the substantially larger expansion velocity in the model B. Given disparity makes large distance ( $d > 2$  kpc) highly unrealistic.

#### 4. Modelling radio emission

The spectrum and high brightness temperature of the radio emission of nova CI Cam 1998 show that the radiation has a synchrotron origin, while the structure and kinematics of the radio source indicates that the emission originates from the shock wave propagating in the CS gas (Mioduszewski & Rupen 2004). The theory of the electron acceleration and generation of magnetic field in the shock wave cannot confidently predict parameters that define the radio emission. I therefore use a parametric description.

Below we assume that the magnetic field and relativistic electrons are homogeneously distributed on average behind the shock front within the layer of  $h = 0.2R$  where  $R$  is the

shock radius. The equipartition between magnetic field and cosmic rays with the electron-to-proton ratio  $K_{ep} = 0.01$  is adopted. The ratio of the relativistic energy (magnetic field plus cosmic rays) to the internal energy in the shock wave ( $\epsilon_r$ ) is a free parameter. The power spectrum of relativistic electrons in the energy range  $E > E_{min} = 0.5$  MeV is assumed  $dN/dE \propto E^{-p}$ , where spectral index  $p$  is a free parameter. The model takes into account the SSA, the  $ff$ -absorption in the fully ionized wind with the temperature  $10^4$  K; the Razin effect is also taken into account. The latter results in the exponential suppression of the spectrum at low frequencies  $\nu < \nu_R$ , where  $\nu_R = (2/3)\nu_p^2/\nu_B$  ( $\nu_p$  is the plasma frequency,  $\nu_B$  is the gyrofrequency). The Razin effect can be taken into account using the flux prefactor (cf. Simon 1969)

$$G = C(\nu) \exp [-(3/2)^{1/2}\nu_R/\nu], \quad (2)$$

where  $C(\nu) = 1$  for  $\nu \geq \nu_R$  and  $C(\nu) = (\nu/\nu_R)^{(3/2-p)}$  for  $\nu < \nu_R$ . The modelling shows that the  $ff$ -absorption and Razin effect are of little importance compared to the SSA.

Preceding results, let us show that a homogeneous distribution of the radio-emitting material in the shell is inconsistent with the observational data. It is well known that the angular size or linear size (if the distance is available) of the opaque radio source can be well determined from the flux (Sligh 1963). The size thus obtained weakly depends on the magnetic field. Assuming the equipartition one can exclude the magnetic field; moreover the size turns out to be insensitive to the ratio of magnetic field and relativistic electrons energy density (cf. Chevalier 1998). The dependence of the synchrotron luminosity at 2.25 GHz of the expanding source in the luminosity maximum on the peak time  $t_m$  is shown in Fig. 3. This diagram is similar to that used for the analysis of radio supernovae (Chevalier 1998). The plot demonstrates that for the shell with the homogeneous brightness the observed monochromatic luminosity of CI Cam 1998 in the maximum on day 5 at the distance  $2 \leq d \leq 5$  kpc corresponds to the expansion velocity  $700 - 1600$  km s<sup>-1</sup>, significantly lower compared to the observed value  $\sim 4000 - 6000$  km s<sup>-1</sup> at this epoch (Fig. 1a). This disparity means that the brightness distribution should be essentially inhomogeneous, i.e. the source has a cloudy structure. Note that the inhomogeneity of the radio brightness of CI Cam 1998 is apparent from the radio image (Mioduszewski & Rupen 2004).

The description of the inhomogeneous radio source requires additional parameters: filling factor ( $f$ ) and the ratio of the cloud radius to the width of the radio-emitting shell ( $\xi = a/h$ ). The intensity of the emergent radiation is then determined by the expressions

$$I_\nu = S_\nu[1 - \exp(-\tau_{\text{eff}})], \quad \tau_{\text{eff}} = \tau_g[1 - \exp(-\tau_c)], \quad (3)$$

where  $S = j_\nu/k_\nu$  is the source function,  $\tau_g = (3/4)(f/\xi)$  is the occultation optical depth (i.e., the average cloud number along the radius),  $\tau_c = (4/3)ak_\nu$  is the average optical depth

of the cloud. The surface fraction covered by clouds (covering factor) is  $1 - \exp(-\tau_g)$ . The expression (3) is used for the flux computation, which is sensible approximation.

The sensitivity of the radio flux behavior to the major parameters is shown in Fig. 4. The reference model A is characterized by  $\epsilon_r = 0.45$ ,  $f = 0.025$ , and  $\xi = a/h = 0.5$ ; three other cases show models in which each parameter is twice as smaller. The reduction of  $\epsilon_r$  decreases the flux at the optically thin stage and shifts the maximum towards the earlier epoch; the reduction of  $f$  decreases the flux in all frequencies; the reduction of  $\xi$  shifts the maximum towards the earlier epoch since the cloud optical depth decreases. In the latter case the flux at the opaque stage is higher because the covering factor gets larger. This plot shows how one can recover the optimal model via parameter variations.

The simulation results for the models A and B are shown in Fig. 5, while the parameter values are given in Table 1. In both models the relative cloud radius is assumed to be  $\xi = 0.5$  in order to secure maximal SSA for the moderate parameter  $\epsilon_r$ . Even with this prerequisite the required fraction of relativistic component is rather high  $\epsilon_r = 0.45$  and  $0.23$  in models A and B respectively. As a result, the shock compression factor turns out to be  $> 4$  so the fraction of the thermal pressure becomes notably lower than unity (Drury & Völk 1981; Chevalier 1983); this fact is taken into account for the calculation of the ion and electron temperatures. The filling factor  $f \approx 0.025$  in both models while the covering factor  $\sim 0.1$  (front and rear sides of the shell are included). Models satisfactorily reproduce the flux evolution at different frequencies, although at late stage the flux decreases more rapidly compared to the observations. Maximum at 2.25 GHz is fully determined by the SSA whereas the optical depth due to  $ff$ -absorption is only 0.15 at  $t = 1$  d. The brightness temperature of radio-emitting clouds at 2.25 GHz in the flux maximum is  $\sim 2 \times 10^{10}$  K, markedly lower than the Compton limit  $\sim 10^{12}$  K.

The relativistic energy fraction  $\epsilon_r$  in the preferred model A is rather high (0.45). This means that the kinetic energy in this model is close to the minimal permissible value. On the other hand, the energy of the model A cannot be significantly larger because otherwise we would come to the large X-ray luminosity. The recovered parameters of the model A therefore are close to the optimal values for the spherical models.

## 5. Nonspherical model

The bipolar structure of the CI Cam 1998 radio map at late times (Mioduszewski & Rupen 2004) indicates that CSM might have two-component structure, e.g., rarefied medium in polar directions combined with the dense equatorial disk. In this picture the radio emission

could be associated with the fast shock waves running in the polar directions, while X-rays are presumably emitted by slow shocks propagating in the dense equatorial disk. Filippova et al. (2008) already proposed the equatorial disk for the interpretation of X-ray emission of CI Cam 1998. This model is preferred compared to the spherical one because it is able to provide the fast decay of the X-ray flux. The ready scenario for the formation of the proposed structure of the CSM is absent. However, one could think that the combination of the slow wind with the velocity of  $32 \text{ km s}^{-1}$  and of the fast disk wind with the velocity of  $\sim 10^3 \text{ km s}^{-1}$  taken together with the gravitation perturbation from the unseen component with the orbital velocity of  $230 \text{ km s}^{-1}$  (Barsukova et al. 2006) might maintain the suggested structure of the CSM.

To simulate the radio and X-ray emission we consider the CSM composed of the rarefied bipolar outflow in cones with the opening angle  $2\theta_0$  and dense equatorial disk with the polar angle range  $\theta_0 < \theta < \pi - \theta_0$ , where  $\theta$  is counted from the polar axis  $z$ . The density in polar cones is constant ( $\rho_0$ ) for  $r \leq r_0 = 2 \times 10^{13} \text{ cm}$  and  $\rho = \rho_0(r_0/r)^2$  for  $r > r_0$ . In the equatorial disk the radial density distribution is similar but values are larger. The disk height over equatorial plane is assumed to be  $z_0 \propto r$  for  $r < r_0$  and  $z_0 = r_0 \cos \theta_0 = \text{constant}$  for  $r \gg r_0$ . This behavior is approximated by the expression

$$z_0 = \frac{rr_0 \cos \theta_0}{r_0 + r}. \quad (4)$$

We assume that the spherical nova shell interacts with the asymmetric CSM described above. The radio and X-ray emission is calculated separately for the polar cones (model Cp) and for the equatorial disk (model Ce) employing the spherically-symmetric model. The total flux is a superposition of both components. The resulting average electron temperature of X-ray-emitting plasma is defined as the flux weighted mean of temperatures of both components. It should be noted, however, that the contribution of X-rays from the bipolar component is small, so the flux and temperature is dominated by the disk shock. Assuming that the expansion of the radio source corresponds to the bipolar shocks we must admit that the inclination angle obeys to the condition  $i > 90^\circ - \theta_0$ .

The nonspherical model describes the X-ray flux and the electron temperature (Fig. 6) significantly better compared to the spherical model A (Fig. 2). Parameters of the CSM for the bipolar cones and the disk are given in Table 1. The X-ray emission is dominated by the disk shock, while the radio is related primarily with the bipolar cones. The relativistic energy fraction is large ( $\epsilon_r = 0.9$ ), so the model energy ( $8 \times 10^{43} \text{ erg}$ ) is close to the minimal value; the initial velocity of the nova shell in the model is  $6300 \text{ km s}^{-1}$ . Interestingly, the recovered energy is only 1.7 times larger than the energy of the spherical model in Filippova et al. (2008) for the case of the Sedov strong explosion models.



Nonspherical model, alleviating the disparity between the model and observed rates of the flux decay, does not remove completely this contradiction. The similar contradiction is present in the disk model of Filippova et al. (2008). The fast decay of the observed X-ray flux may be related with another effect being absent in the disk shock model, namely, the spherization of the post-shock flow due to outflow of shocked gas perpendicular to the equatorial plane. However, to take into account this effect requires the multi-dimensional hydrodynamics.

The study of possible uncertainties implies that the nova energy and the density of the CSM are determined in our model with the accuracy of about 30%. The mass of the nova shell is less certain because results weakly depend on the mass for the fixed value of energy. The optimal mass range  $(1 - 5) \times 10^{-7} M_{\odot}$  is determined from the requirement of the description of the early ( $t \approx 2$ ) expansion. Finally, it should be stressed that the proposed nonspherical model is illustrative; the actual distribution of the CSM may somewhat differ from the recovered optimal model.

## 6. Discussion

Our goal was the possibility to account for the radio and X-ray emission from nova CI Cam 1998 in the framework of a unified model of the nova shell interaction with the CSM. I show that the interaction of the spherical nova shell with the spherical CSM is able to describe the the evolution of the radio flux and the expansion kinematics of the radio source and only roughly to describe the X-ray emission assuming the distance of 2 kpc. The larger distance is less likely because it suggests the larger expansion velocity of the radio source and thus more harder X-ray spectrum in odd with observations. For the distance of 2 kpc, however, more reasonable description can be found in the model of the interaction of the spherical shell with the nonspherical CSM. The latter is composed by the combination of the rarefied bipolar outflow and the dense equatorial disk.

The rarefied gas in bipolar cones can be associated with the fast bipolar wind characteristic of the binary systems with accretion disks. Robinson et al. (2002) report on the detection in the *HST* spectra taken in March 2000 of the ultraviolet lines of C IV and Si IV with P Cygni profiles and the expansion velocities of  $\sim -1000 \text{ km s}^{-1}$  in the blue absorption wing. With this velocity and wind density from Table 1 the mass loss rate related with the bipolar outflow is then  $\sim 2.4 \times 10^{-6} M_{\odot} \text{ yr}^{-1}$ . For the equatorial wind velocity  $32 \text{ km s}^{-1}$  (Robinson et al. 2002) the mass loss rate related with the equatorial wind turns out to be  $\sim 0.5 \times 10^{-6} M_{\odot} \text{ yr}^{-1}$ . The total mass loss rate is therefore  $\sim 3 \times 10^{-6} M_{\odot} \text{ yr}^{-1}$ , close to  $\sim (1 - 2) \times 10^{-6} M_{\odot} \text{ yr}^{-1}$  obtained for the spherical model of X-ray emission of CI Cam

1998 (Filippova et al. 2008).

Given the opening angle of bipolar outflow  $\sim 120^\circ$  the inclination angle of the binary system should be  $i > 30^\circ$  to meet requirement that the shock tangential velocity should coincide with the physical expansion velocity. This inequality is consistent with another inequality  $i > 38^\circ$  found earlier from the requirement that the unseen component of the binary is the white dwarf (Barsukova et al. 2006).

Parameters of the optimal model of the nova CI Cam 1998  $E \sim 8 \times 10^{43}$   $M \sim (1 - 5) \times 10^{-7} M_\odot$ , bipolar structure, and the expansion velocity  $\sim 6300$  km s $^{-1}$  are reminiscent of the similar properties of recurrent nova RS Oph 2006. Recently Rupen et al. (2008) studied bipolar structure of the radio source of RS Oph 2006 and found that the expansion velocity of bipolar shocks is  $\sim 10^4$  km s $^{-1}$ . They estimate the energy of bipolar outflow of RS Oph 2006 to be  $\sim 10^{44}$  erg, which is close to the energy of CI Cam 1998; the estimated ejecta mass  $\sim 10^{-7} M_\odot$  of RS Oph 2006 is also close to the shell mass of CI Cam 1998.

Yet there are some apparent differences between these novae. For comparable distances ( $\sim 2$ ) kpc and comparable extinction ( $A_V \sim 2.5$  mag) the optical flux in  $V$  band at maximum of CI Cam 1998 is  $\sim 40$  times lower compared to RS Oph 2006. On the other hand the X-ray flux of CI Cam 1998 in 0.5-10 keV band is  $\sim 20$  times larger, while radio flux at 5 GHz is  $\sim 7$  larger compared to RS Oph 2006. Binary systems are dissimilar as well. For CI Cam the binary period is 19 d and the donor is B-giant with the mass  $\geq 12 M_\odot$  (Barsukova et al. 2006), whereas for RS Oph the binary period is 460 d and the donor is M-giant with the mass  $\approx 0.5 M_\odot$  (Dobrzycka & Kenyon 1994). All these differences leave open the issue of the possible similarity of the outburst physics of CI Cam 1998 and RS Oph 2006.

## REFERENCES

- Althaus, L. G. et al. 2005, A&A, 441, 689
- Barsukova, E. A. et al. 2006, ASP Conference Series, Vol. 355, 305
- Belloni, T. et al. 1999, ApJ, 527, 345
- Chevalier, R. A. 1983, ApJ, 272, 765
- Chevalier, R. A. 1998, 499, 810
- Clark, J. S. et al. 2000, A&A, 356, 50
- Dobrzycka, D. & Kenyon, G. J. 1994, AJ, 108, 2259

- Drury, L. O’C. & Voelk, J. H. 1981, *ApJ*, 248, 344
- Garcia, M. R. et al. 1998, *IAU Circ.* 6865
- Filippova, E. V., Revnivitsev, M. G., & Lutovinov, A. A. 2008, *AstL*, 34, 797
- Filippova, E. V., Revnivitsev, M. G., & Lutovinov, A. A. 2009, *AstL*, 35, 688
- Frontera, F. et al. 1998, *A&A* 339, L69
- Hjellming, R. M. 1998, *IAU Circ.* 6862
- Ishida, M., Morio, K., & Ueda, Y. 2004, *ApJ*, 601, 1088
- Kato, M. & Hachisu, M. I. 1994, *ApJ*, 437, 802
- Mioduszewski, A. J. & Rupen, M. P. 2004, *ApJ*, 615, 432
- Prialnik, D. 1986, *ApJ*, 310, 222
- Revnivitsev, M. G., Emelyanov, A. N., & Borozdin, K. N. 1999, *AstL*, 25, 294
- Robinson, E. L., Ivans, I. I. & Welsh, W. F. 2002, *ApJ*, 565, 1169
- Rupen, M. P., Mioduszewski, A. J., & Sokoloski, J. L. 2008, *ApJ*, 688, 559
- Simon, M. 1969, *ApJ*, 156, 341
- Slish, V. I. 1963, *Nature* 199, 682
- Smith, D. et al. 1998, *IAU Circ.* 6855
- Spitzer, L. Jr. *Physics of fully ionized gases.* (Interscience Publ., New York, 1962)
- Sutherland, R. S. & Dopita, M. A. 1993, *ApJS*, 88, 253
- Wagner R. M. & Starrfield S. G. 1998, *IAU Circ.* 6857

Table 1: Model parameters

Model	$d$ kpc	$M$ $10^{-7} M_{\odot}$	$E$ $10^{44}$ erg	$\rho_0$ $10^{-15}$ g cm $^{-3}$	$\epsilon_r$	$p$	$f$
A	2	2	1.1	2	0.45	2.3	0.025
B	5	2	16	3.2	0.23	2.3	0.025
Cp	2	2	0.8	0.6	0.9	2.1	0.04
Ce	2	2	0.8	4	0.27	2.1	0.04

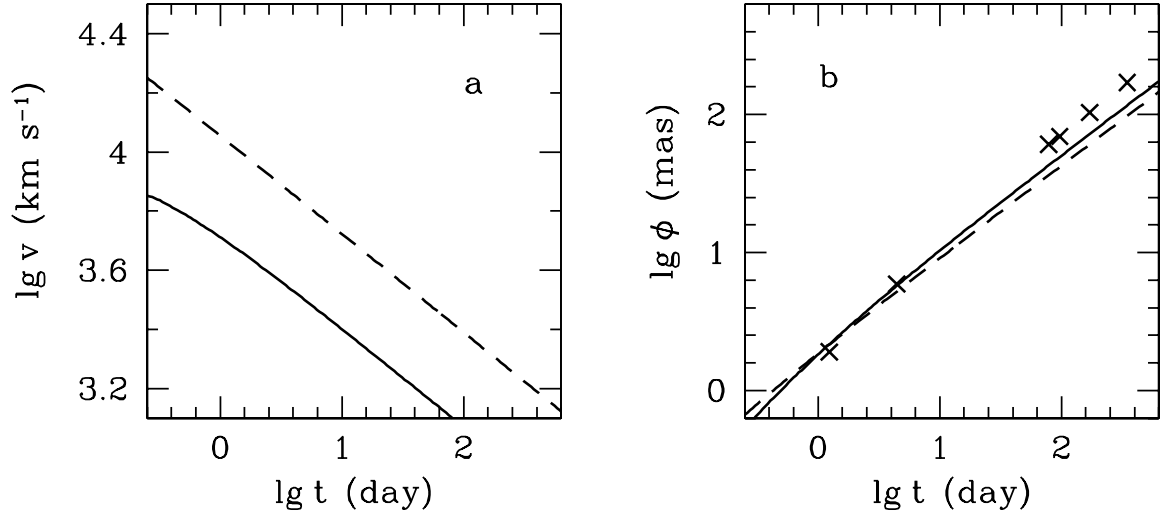


Fig. 1.— Evolution of the velocity and angular radius of the shock wave of CI Cam 1998 in the model of the nova shell interaction with CSM. Left (*a*): the velocity in the model A (*solid line*) and in the model B (*dashed line*). Right (*b*): the angular radius in the model A (*solid line*) and in the model B (*dashed line*). Interferometric data (*crosses*) are taken from (Mioduszewski & Rupen 2004).

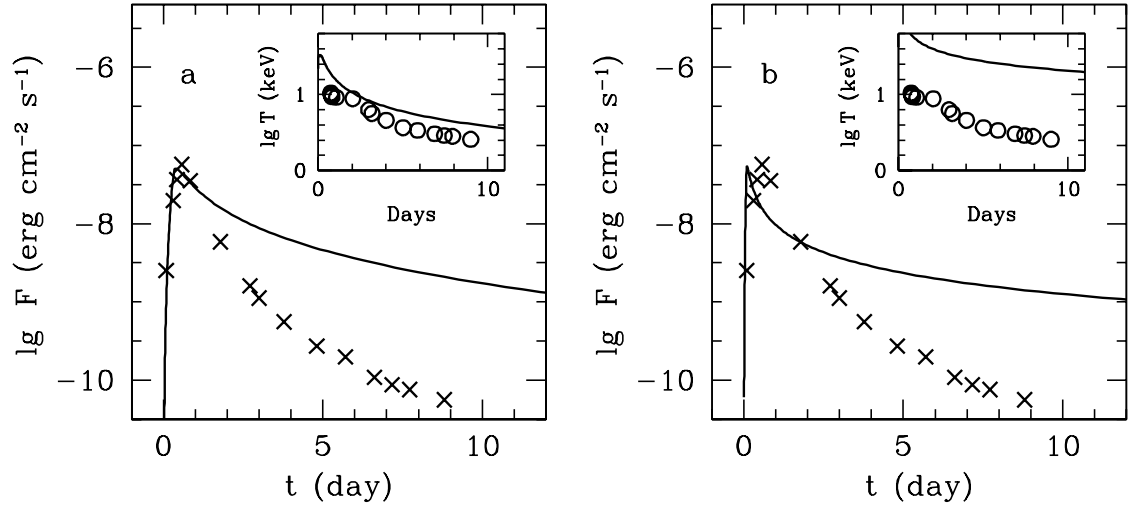


Fig. 2.— X-ray flux in 3-20 keV band in the model A (a) and model B (b) compared with the observational data (Filippova et al. 2008) (*crosses*). Insets show electron temperature in the model (*line*) and observations (Filippova et al. 2008).

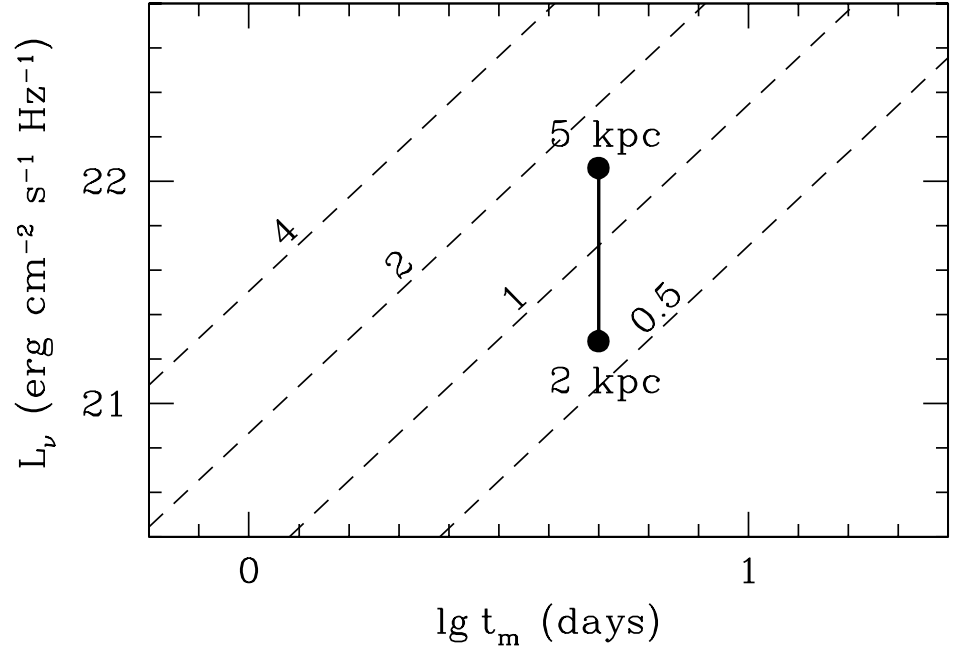


Fig. 3.— Peak synchrotron luminosity of the expanding spherical shell vs. time of the peak at the frequency 2 GHz. Numbers at the lines indicate the velocity in units of  $1000 \text{ km s}^{-1}$ .

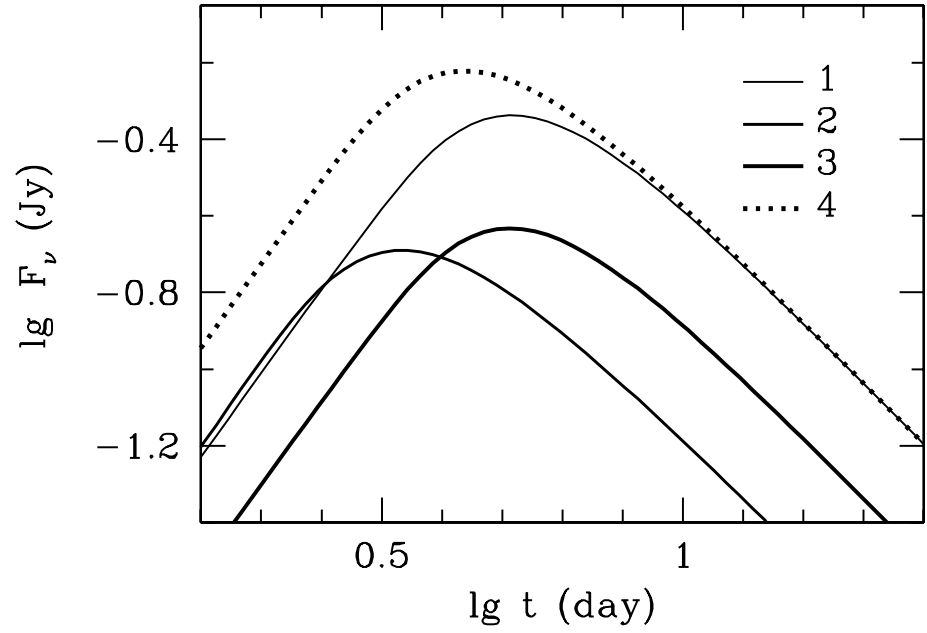


Fig. 4.— Flux evolution at 2 GHz for the expanding clumpy spherical shell. 1 – standard model (see text); 2 – density of the relativistic component is twice as smaller; 3 – filling factor is twice as smaller; 4 – cloud size is twice as smaller.



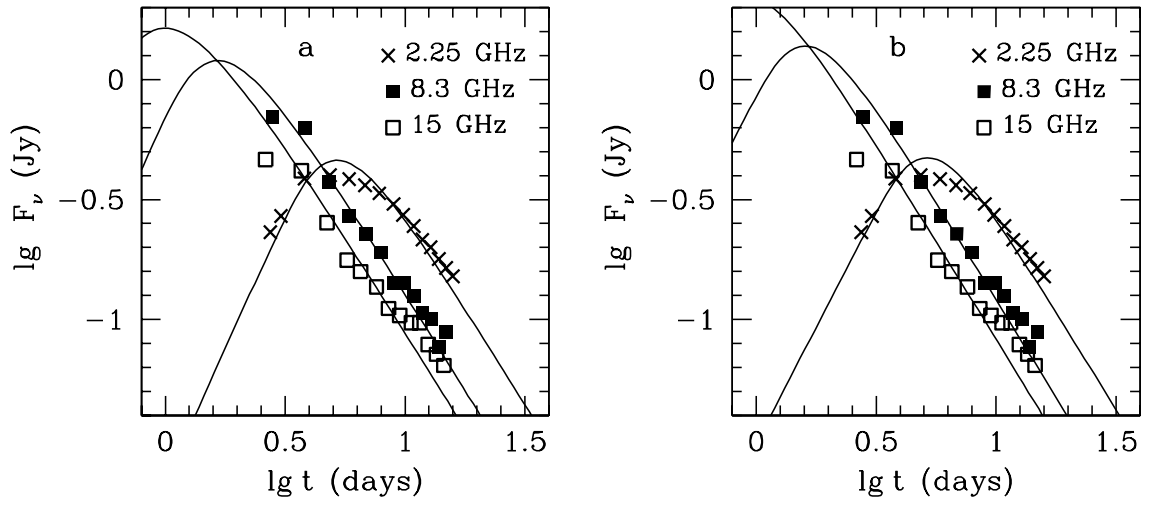


Fig. 5.— Flux evolution at frequencies 2 GHz, 8 GHz, and 15 GHz in the model A (*a*) and model B (*b*) compared to data (Clark et al. 2000).

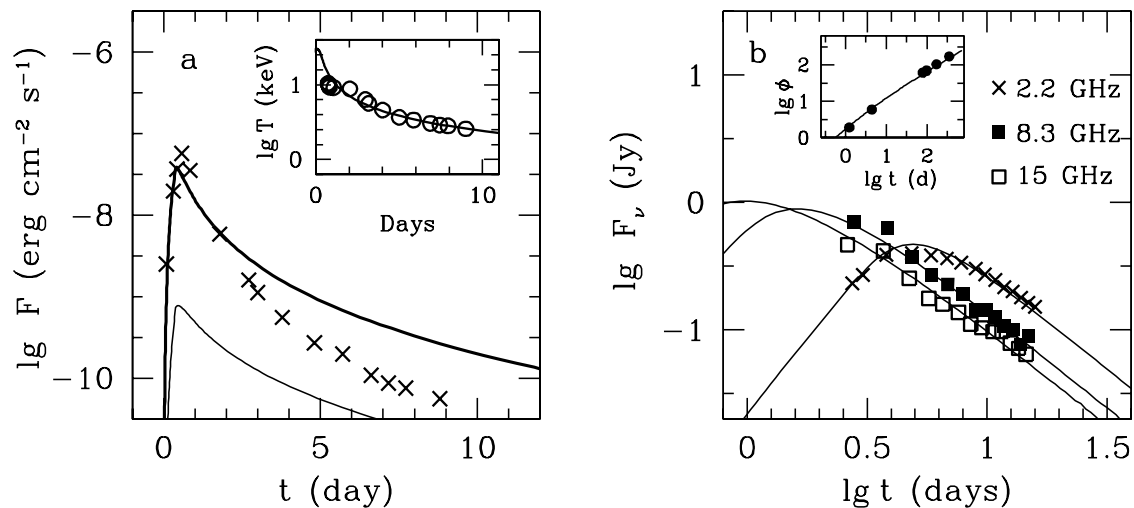


Fig. 6.— Evolution of X-ray and radio emission in the nonspherical model of CSM compared with data. Left (a): the same as in Fig. 2 but for nonspherical model; shown are the total flux (*thick line*) and contribution of shocks in polar cones (*thin line*). Right (b): the same as in Fig. 5 but for nonspherical model. The inset shows evolution of the angular radius (in mas) of the polar shock.